Potential Electrochemical Coronary Artery Disease Diagnosis Based on A Periostin Immunoassay

Xiu-Feng Zheng[1], Yuan-Yuan Wang[2], Lei Han[3], Xi-Chun Wang[4], Shi-Lei Zhao[5] and Hui Zou[1]*

[1] Department of Cardiology, Heilongjiang Hospital, Harbin, Heilongjiang, P.R. China.
[2] Department of Cardiology. Mudanjiang Medical University Hongqi Hospital, Mudanjiang, Heilongjiang, P.R. China.
[3] Department of Respiratory. Mudanjiang Medical University Hongqi Hospital, Mudanjiang, Heilongjiang, P.R. China.
[4] Department of Gerontological Neurology, Heilongjiang Hospital, Harbin, Heilongjiang, P.R. China.
[5] Department of Nephrology, The First Affiliated Hospital of Harbin Medical University, Harbin, Heilongjiang, P.R.China
[*] E-mail: 87888829@qq.com

The preparation of a sensitive amperometric immunosensor for periostin was achieved. The synthesis of golg nanoprobe was carried out through depositing the gold nanoparticles in situ on silica nanophere functionalized by polydopamine, which was followed to label the signal antibodies. The method of covalent immobilization, in which the antibodies were captured on the glassy carbon electrode, was employed for the preparation of the immunosensor. The cyclic voltammetry (CV) was employed to investigate the performance of the decorated electrode at different modification stages. Furthermore, the study of the performance of the immunosensor was carried out in detail. The prepared immunosensor demonstrates highly sensitive for periostin detection with excellent correlation of detection ranging from 0.1 to 150.0 ng/mL, where limit of 0.06 ng/mL can be detected, and estimated through a signal-to-noise ratio of 3. The periostin be detected by one-step immunoassay in the proposed method, which acts as valuable role to diagnose the clinical early coronary artery disease.

1. INTRODUCTION

A main cause of death and disease is coronary artery disease (CAD), which is increasing rapidly in the developing countries. Elucidating the pathogenesis and identifying the CAD risk, is still a huge challenge. It is famous that the main CAD pathophysiological mechanisms of are underlay by

the atherosclerosis, and recently angiogenesis has been viewed as a key to develop the atherosclerosis [1-3]. The plaque angiogenesis is mainly regulated by the vascular endothelial growth factor (VEGF). It could facilitate the growth of plaque and play a presumed role in the instability of plaque [4], where the influences are spreadedvia the kinase domain receptor [5]. Thus, the control of the VEGF/kinase insert domain receptor (KDR) signaling pathway might be essential for the angiogenesis and the repairmen of vessel, which is related to CAD pathogenesis [6]. Periostin, which is an extracellular matrix (ECM) belonging to the group of fascilin, play a role in cell adhesion, differentiation and migration [7]. Periostin was demonstrated by Bagnato that it may serve as a potential migratory stimulus in neointima and further affect the human atherosclerosis [8]. However, the mechanisms of the periostin induced up-regulation as well as the probable effect for the atherosclerotic vascular disease are still ambiguous. According to some researches, the up-regulation of KDR in the human microvascular endothelial cells and the breast cancer was caused by periostin [9, 10]. Besides, it was demonstrated that KDR could affect atherosclerosis by the control of the VEGF/KDR signaling pathway. Thus, it is crucial to develop a proper approach to determine periostin. Recently, owing to the low dielectric, low density constant, low refractive, good biocompatibility, large surface area and uniform pore size, researchers have been focusing on the mesoporous materials [11-14]. MS (mesoporous silica) demonstrates the characteristics of both silica and mesoporous materials, which makes itself significant. Some other materials, such as noble metal and fluorescence molecules, can be combined with silica due to the versatility of its chemistry [15-18]. Bearing this in mind, targeted drug delivery and nano-carriers in the drug transport can be achieved by the wide use of the functionalized mesoporous silica (MS) [19, 20].

To obtain highly sensitive immunosensors, signal amplification is also very vital. As the signal transduction tools in the immunoassays, Au NPs (Au nanoparticles) which is labeled with antibodies are used commonly [21, 22]. Owing to its good biocompatibility, large specific surface area and high surface free energy, the antibody can be firmly adsorbed by Au NPs [23, 24]. Dopamine, acting as an chemical messenger in mammalians, is a vital catecholaminergic neurotransmitter and demonstrates very crucial to physiological issue [25]. As shown in recent research, one layer of polydopamine (PDA) can be spontaneously formed on virtually any surface due to its self-polymerization at weakly alkaline condition [26-28]. Therefore, an extremely versatile platform can be provided by this PDA functionalization not only for possibly depositing metallic nanoparticles in situ but also for immobilizing the biological molecules [29-31].

The gold nanoprobe was successfully achieved by depositing Au nanoparticles on silica decorated by PDA, and it was followed to label the signal antibodies. The receptor molecules total amount, which is anchored on surface of the sensor, can determined the sensitivity of the immunosensor. A larger amount of anchoredreceptor molecules were allowed for due to the enlargement of the sensor area, which led to increase the binding capacity. Thus, in our work, the glassy carbon electrode (GCE) decorated by MS-Au NPs increased the amount of the antibody loaded to promote the sensitivity of the immunosensor.

2. EXPERIMENTS

2.1. Reagent

We purchase the anti-periostin and periostin from Biocell Company (Zhengzhou, China). From Sigma, dopamine, human serum albumin (HSA), $HAuCl_4$ and Bovine serum albumin (BSA, 96–99%) were purchased. mixing the stock solutions of 50 mM NaH_2PO_4 and Na_2HPO_4, made the phosphate-buffered saline (designated as PBS) successfully fabricated with pH 7.4. containing 2% (w/v) Tween-20 (PBST), A PBS (pH=7.4, 50ml) which was employed to act as rinsing buffer. Containing 0.05% (w/v) BSA, A PBS (50ml, pH=7.4) which c was taken as hindering solution. Additionally, a Tris–HCl buffer (pH=8.5, 50ml) was fabricated to make functionalization of PDA.

2.2 Apparatus

A CHI 660 electrochemical workstation (CH Instruments, USA) was employed to perform all electrochemical immunoassay. A saturated calomel reference electrode (SCE), the modified electrode which is working electrode, a platinum wire auxiliary electrode constituted the three-compartment electrochemical cell. The JEOL 1010 TEM was used.*Preparation of gold nanoprobe.*

2.3. Preparation of gold nanoprobe

The following description is the preparation procedure of Au nanoprobe: First of all, according to the previous research, monodispersed silica nanosphere was fabricated [32]. Then, by depositing gold nanoparticles on PDA/silica surface in situ, gold nanoparticles with nanocomposite of decorated PDA/silica was synthesized. In brief, before stirring the mixture for 5 hours at room temperature, dopamine (5 mg) was taken into 5.0 mg/mL of 1ml dispersion of silica nanosphere (with pH=8.5 50 mM Tris–HCl buffer).. After centrifugation with rinsing three times with water, as-prepared PDA/silica was dispersed again in $HAuCl_4$ solution (2.0 mL, 10 mg citrate contained) of 0.25% (w/v)., and then another 2 hours for stirring was needed. After one more cycle of rinsing three times with water and centrifugation , the gold nanoparticles which were on decorated PDA/silica were achieved and dispersed in water (2.0 ml) for coming use.

2.4. Fabrication of the immunosensor

The 1.0, 0.3 and 0.05 μm alumina slurries were employed to polish the GCE (diam = 4 mm) and remove adsorbed organic matter on micro cloth pad to a mirror-like finish. After removing the trace alumina on the surface of electrode, water and ethanol were used to clean the electrode in the ultrasonic bath, then it can be admitted to dry at room temperature. 25 ul solution of gold NPs-silica composite was pipetted onto the GCE surface. The casting solution was agreed to dry overnight at 4 °C. Then, the water was employed to rinse the decorated electrode (Au NPs-silica/GCE), which was followed to be immersed into the anti-periostin solution for 12 hours at 4 °C. Lastly, to avoid the non-

specific adsorption and block possible remaining active sites, BSA solution (w/w, 0.25%) was used to incubate the obtained electrode at 35 °C for about 1 hour. The finished immunosensor should be stored at 4 °C when not in use.

2.5. Experimental measurements

An unstirred electrochemical cell was the place where electrochemical measurements were performed at 35 °C and the scan rate is 50 mV/s with the potential sweep vs SCE ranging from -0.2 to 0.6 V . The method, in which the immunosensor was in PBS (0.01 M) including different concentrations of periostin (pH was equal to7.0) for 20 min at 35 °C, was employed to perform the immunoreaction. The response fluctuation of oxidation current (ΔI) before and after the immunoreaction in the solution of $[Fe(CN)_6]^{4-/3-}$ (5.0 mM , pH is equal to 7.0),where 0.1 M KCl was contained, can be detected to determine the periostin level.

3. RESULTS AND DISCUSSION

In this work, the key for one layer of multifunctional PDA film coating on the silica nanosphere surface and the subsequent depositing gold nanoparticles in situwas definite self-polymerization of dopamine. The morphology of the as-synthesized Au NPs decorated nanocomposite of PDA/silica was characterized by TEM. As shown in Fig. 1A, compared with naked silica, PDA/silica diameter was increased for 50 nm . This suggests that the dopamine oxidative self-polymerizing successfully made one layer of PDA film formed. $AuCl_4^-$ adsorbed on PDA film surface can be reduced to form gold nanoparticles with adding no more reducing agent in situ due to abundant catechol groups on its surface. As shown in Fig. 1B, this idea can be proved by the TEM. After reducing it with chemical method in situ, numerous highly dispersed nanoparticles were observed, which were about an average size of about 120 nm. This phenomenon suggested that gold nanoparticles decorated nanocomposite with PDA/silica was successfully formed.
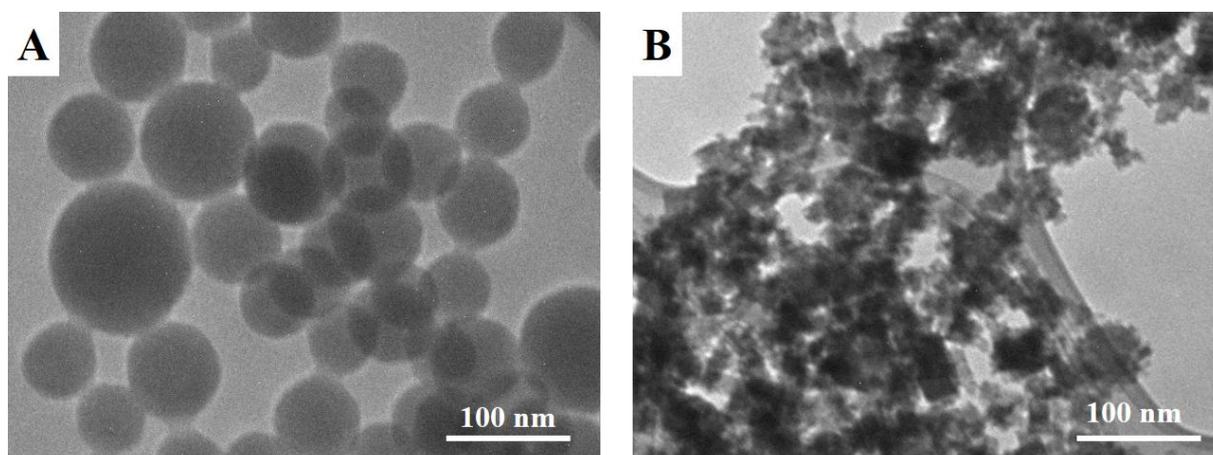
Figure 1. (A) TEM images of PDA/silica, (B) TEM images of as-synthesized nanocomposite of Au NPs decorated on PDA/silica.

Forming gold nanoparticles on the PDA/silica surfacewas characterized by UV–vis spectroscopy. Absorption peak can't be detected in the PDA/silica in Fig. 2A. However, owing to the formation of an colloidal gold nanoparticles synthesized through the traditional method of citrate reduction [33], an obvious 504 nm absorption peak was observed after reducing it with chemical way in situ, which was obviously identified as the plasmon absorption peak of colloidal gold nanoparticles. The surface influence of depositing gold nanoparticles on the core/shell nanosphere is to lead little red-shift of the highest absorption peak. The slight red-shift of the maximum absorption peak caused by the surface effect of Au NPs deposited on the core/shell nanosphere is in agreement with the result in the previous similar report [34]. In addition, after depositing gold nanoparticles on the PDA/silica surface in situ, the presence of gold is proved by the EDX spectrum as shown in Fig. 2B. The nanocomposite of gold nanoparticle decorated on PDA/silica was confirmed through these results of the measurements. A new Au nanoprobe for the nonenzymatic electrochemical immunoassay was synthesized by the inherent interaction between antibody biomolecules and Au nanoparticles. This in-situ deposition method can be employed as a method to not only proves the controllability and repeatability for preparing the gold nanoprobe but also loads high-content Au nanoparticles in a simple and green way.
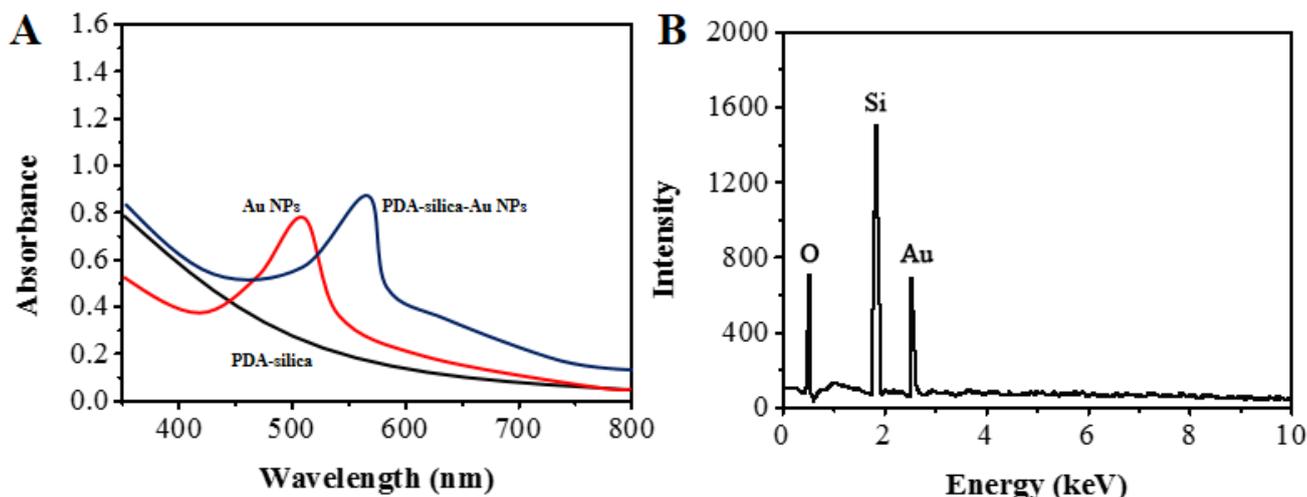

Figure 2. (A) UV-vis spectrum of synthesized nanocomposite of gold nanoparticle decorated on PDA/silica, Au nanoparticles and PDA/silica. (B) EDX spectra of the obtained nanocomposite of gold nanoparticle decorated on PDA/silica.

Fig. 3 presented the cycle voltammetry data of the various decorated electrodes in $[Fe(CN)_6]^{4-/3-}$ solution (5 mM), which was containing 0.1 M KCl At the bare GCE, a reversible CV was revealed by the labeling redox $Fe(CN)_6^{4-/3-}$. The peak current increased rapidly while gold nanoparticles functionalized PDA/silica nanocomposite decorated the surface of the GCE. The membrane changed to be less conductive, and current response decreased due to the anti-periostin immobilized on the surface of electrode. The decreased current peak is observed when the immunosensor was incubated in the periostin solution for 20 min. The formation of anti-

periostin/periostin immunocomplex contribute to this phenomenon, because it plays a role of inert electron and mass transfer blocking layer, where the ferricyanide diffusing toward the electrode surface is hindered. The additions resist the electron-transfer kinetics of the redox probe at the electrode interface [35]. As a result, the biosensor has been fabricated successfully. These above CV data could be used not only to verify the successful immobilisation of Au NPs, silica and antibody macromolecules onto GCE surface, but also to monitor the changes of electron transfer resistance caused by antigen–antibody reaction [36, 37].
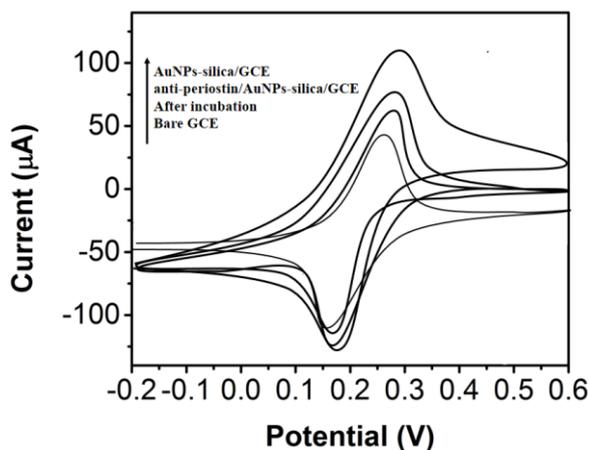

Figure 3. CVs of different stage electrode: anti-periostin/AuNPs-silica/GCE and after pretreated with the solution containing periostin for 20 min, bare GCE. Scan rate, 50 mV/s, Supporting electrolyte: solution of $Fe(CN)_6^{4-/3-}$ (5 mM), where 0.1 M KCl is contained.
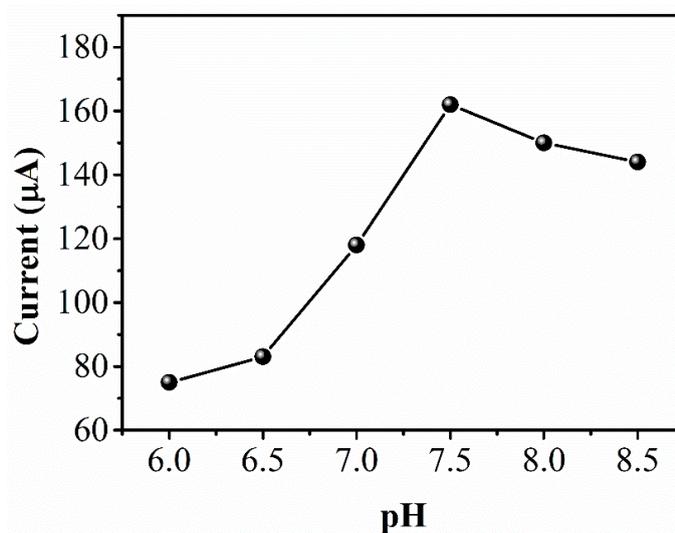
Figure 4. The solution pH Influence on the response of the immunosensor incubated with the presence of periostin (20 ng/ml) in the solution of 5 mM $Fe(CN)_6^{4-/3-}$, where 0.1 M KCl was contained. The scanning rate was 50 mV/s. All potentials are compared with SCE.

The amperometric response of the immunosensor can be affected by the experimental variables, such as the incubation time, the incubation temperature and the pH of supporting electrolyte. Among them, pH value of detection solution has an obvious effect on the performance of immunosensors [38]. As demonstrated in Fig. 4, the influence of solution pH between 6.0 and 8.5 on the immunosensor behavior was investigated, where a maximum value of current response was observed at pH 7.0. Therefore, in the whole study, every experiments was performed in the solution of $Fe(CN)_6^{4-/3-}$, where pH was equal to 7.0.

Immunosensors which was produced through various process were conducted to compare with each other as displayed in Fig. 5. The plots of anti-periostin/AuNPs-silica/GCE and anti-periostin/GCE were displayed by the curves as shown in Fig. 5. The immunosensors demonstrated higher sensitivity (anti-periostin/AuNPs-silica/GCE) and wider dynamic measurement range, which was compared with that of anti-periostin/GCE. The prepared immunosensor demonstrates highly sensitive (778 nA/ng/ml) for detecting periostinwith excellent correlation of detection ranging from 0.1 to 150.0 ng/mL, which has a detection limit of 0.06 ng/mL. The presence of AuNPs-silica not only obviously increased the surface area to capture a large amount of modified antibodies, and enzymes, but also accelerated the electron transfer [39]. The sensitivity of the anti-periostin/AuNPs-silica/GCE was compared with that of other reported modified electrodes and the results were presented in Table 1. This low detection limits might be attributed to the enormous loading of AuNPs which greatly amplified the stripping peak signals.
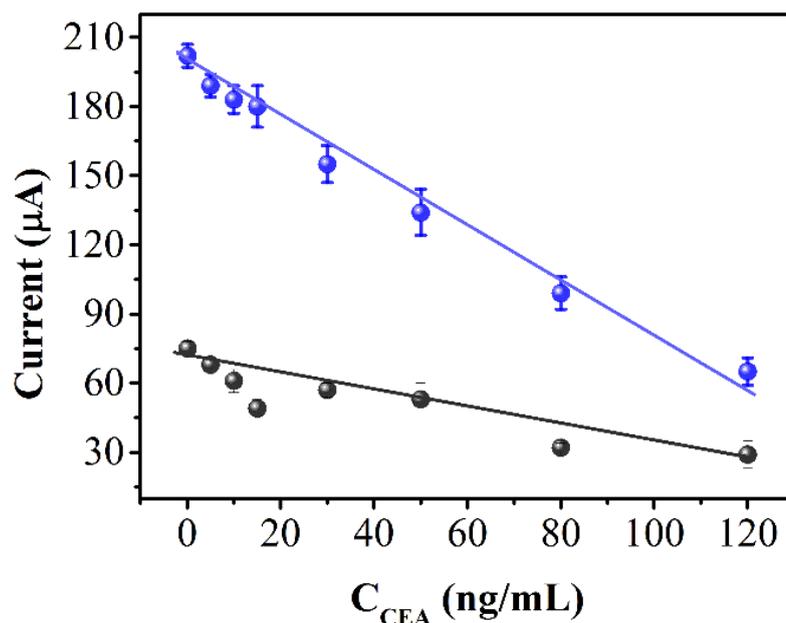
Figure 5. Calibration plots of the anodic peak current response versus concentration of anti-periostin/AuNPs-silica/GCE and anti-periostin/GCE with various immunosensors in optimal conditions. The scanning rate was 50 mV/s. Every potential is compared with SCE.

Table 1. Comparison of the present anti-periostin/AuNPs-silica/GCE with other periostin determination methods.

Electrode	Linear detection range	Detection limit	Reference
Elecsys® periostin immunoassay	10–160 ng/mL	4 ng/mL	[40]
ECL immunoassay	10–160 ng/ml	3 ng/mL	[41]
ARCHITECT® Periostin assay	5.2-73.3 ng/mL	–	[42]
anti-periostin/AuNPs-silica/GCE	0.1 to 150.0 ng/mL	0.06 ng/mL	This work

When samples of human serum is analyzed with no separation, the immunosensor selectivity is vital. With 40 ng/ml periostin, 40 ng/ml hepatitis B surface antigen, 40 ng/ml α-1-fetoprotein and 40 ng/ml hepatitis B core antigen was respectively investigated to the influence of possible interferences in human serum, which was aiming to reaearch the immunosensor selectivity. The peak current responses by CV was found to show less than 4.7% difference, which indicated that the system was highly selective to the periostin. It is worth to note that this technique can be feasible to determine the periostin in human specimens.

One key element in the development and application of immunosensors is the regeneration. By immersing it in solution of the urea solution (4 M) simply for almost 10 minutes and removed to rinse it with using the water, the regeneration of as-prepared immunosensors could be achieved after each experiment. The successive measurements which was repeated eight times were employed to acquire a relative standard deviation (R.S.D.) of 4.6%.

Owing to the leakage of $Fe(CN)_6^{4-/3-}$ mediator and he slow deactivation of protein on the electrode, the state of the decorated electrode was observed to gradually decrease after several cycles of use. To acquire R.S.D. of 3.4%, the measurements with 50 CV in working buffer, was employed, where the study of durability of consecutive assays was carried out. Investigation of long-time immunosensor stability was conducted on 90-day period. The immunosensors could remain the 82.4% and 93.5% of initial after the storing time with 90 days and 60 days at 4 °C respectively, which demonstrated acceptable storage stability. To determine the periostin in human serum for routine clinical early diagnosis of coronary artery disease, the present immunoassay method, where immunosensor displayed acceptable storage stability, is suitable.

Table 2. The comparison of results obtained in serum samples with different methods.

Serum samples	1	2	3	4	5	6
Immunosensor (ng/ml)	0.53	5.02	10.52	24.89	50.36	72.89
ELISA (ng/ml)	0.49	5.11	10.49	22.51	52.19	70.88
Relative deviation (%)	7.2	4.1	5.7	3.6	7.5	4.4

To test the accuracy of periostin, the results coming from five sera by using the well-defined method, was compared with the ELISA, which is a useful and powerful method for serum analysis. Data in Table 2 displayed the relative deviation between two method and the results. The two methods

compared well with each other due to the relative error from comparison of two ideas ranging from 10.3% to -7.1%. Thus, the immunoassays requirement of periostin for clinical early diagnosing coronary artery disease could be satisfied by the present method.

4. CONCLUSIONS

The ultrasensitive electrochemical immunoassay at an immunosensor was carried out by preparing a new Au nanoprobe, which was based on depositing high loading gold nanoparticles in situ on the decorated PDA/silica surface. The controllable and simple method to fabricate new Au nanoprobe is the in-situ deposition. Acceptable accuracy, satisfiable storage stability, low detection limit and high sensitivity are the advantages of the immunosensor. In summary, the practical clinical detection of serum periostin level can be possibly achieved by further developing this proposed method.

References

1. R.L. Silverstein and R.L. Nachman, *Circulation*, 100 (1999) 783.
2. R. Khurana, M. Simons, J.F. Martin and I.C. Zachary, *Circulation*, 112 (2005) 1813.
3. C. Emanueli and P. Madeddu, *British journal of pharmacology*, 133 (2001) 951.
4. B. Doyle and N. Caplice, *Journal of the American College of Cardiology*, 49 (2007) 2073.
5. F. Shalaby, J. Rossant, T.P. Yamaguchi, M. Gertsenstein, X.-F. Wu, M.L. Breitman and A.C. Schuh, *Nature*, 376 (1995) 62.
6. Y. Wang, Y. Zheng, W. Zhang, H. Yu, K. Lou, Y. Zhang, Q. Qin, B. Zhao, Y. Yang and R. Hui, *Journal of the American College of Cardiology*, 50 (2007) 760.
7. J. Litvin, A.H. Selim, M.O. Montgomery, K. Lehmann, M.C. Rico, H. Devlin, D.P. Bednarik and F.F. Safadi, *Journal of cellular biochemistry*, 92 (2004) 1044.
8. C. Bagnato, J. Thumar, V. Mayya, S.-I. Hwang, H. Zebroski, K.P. Claffey, C. Haudenschild, J.K. Eng, D.H. Lundgren and D.K. Han, *Molecular & Cellular Proteomics*, 6 (2007) 1088.
9. R. Shao and X. Guo, *Biochemical and biophysical research communications*, 321 (2004) 788.
10. A. Försti, Q. Jin, A. Altieri, R. Johansson, K. Wagner, K. Enquist, E. Grzybowska, J. Pamula, W. Pekala and G. Hallmans, *Breast cancer research and treatment*, 101 (2007) 83.
11. S. El Sayed, M. Milani, C. Milanese, M. Licchelli, R. Martínez‐Máñez and F. Sancenón, *Chemistry-A European Journal*, 22 (2016) 13935.
12. B. Li, X. Li, W. Li, Y. Wang, E. Uchaker, Y. Pei, X. Cao, S. Li, B. Huang and G. Cao, *ChemNanoMat*, 2 (2016) 281.
13. M. Colilla, A. Baeza and M. Vallet‐Regí, *The Sol-Gel Handbook-Synthesis, Characterization, and Applications: Synthesis, Characterization and Applications, 3-Volume Set*, (2015) 1309.
14. J.L. Vivero-Escoto, Y.-D. Chiang, K. Wu and Y. Yamauchi, *Science and Technology of Advanced Materials*, 13 (2012) 33.
15. D. Balogh, M.A. Aleman Garcia, H.B. Albada and I. Willner, *Angewandte Chemie*, 127 (2015) 11818.

16. M. Qasim, B.R. Singh, A. Naqvi, P. Paik and D. Das, *Nanotechnology*, 26 (2015) 285102.
17. X. Wang, H. Wang, M. Lu, X. Ma, P. Huang, X. Lu and X. Du, *Journal of separation science*, 39 (2016) 1734.
18. T. Kamegawa, Y. Ishiguro, Y. Magatani and H. Yamashita, *Journal of Nanoscience and Nanotechnology*, 16 (2016) 9
19. ang, S. Ye and A. Yao, *Journal of the Chinese Ceramic Society*, 41 (2013) 281.
20. M. Catauro, F. Papale, G. Roviello, C. Ferone, F. Bollino, M. Trifuoggi and C. Aurilio, *Journal of Biomedical Materials Research Part A*, 102 (2014) 3087.
21. D. Wang, N. Gan, H. Zhang, T. Li, L. Qiao, Y. Cao, X. Su and S. Jiang, *Biosensors and Bioelectronics*, 65 (2015) 78.
22. K. Chen, Z. Lu, Y. Qin and G. Jie, *Journal of Electroanalytical Chemistry*, 754 (2015) 160.
23. L. Wang, J. Shan, F. Feng and Z. Ma, *Anal. Chim. Acta.*, 911 (2016) 108.
24. L. Jiao, Z. Mu, C. Zhu, Q. Wei, H. Li, D. Du and Y. Lin, *Sensors and Actuators B: Chemical*, 231 (2016) 513.
25. Y. Li, H. Dai, Q. Zhang, S. Zhang, S. Chen, Z. Hong and Y. Lin, *Journal of Materials Chemistry B*, 4 (2016) 2591.
26. Y. Liu, K. Ai and L. Lu, *Chemical Reviews*, 114 (2014) 5057.
27. J. Cui, Y. Ju, K. Liang, H. Ejima, S. Lörcher, K.T. Gause, J.J. Richardson and F. Caruso, *Soft Matter*, 10 (2014) 2656.
28. J. Fu, Z. Chen, M. Wang, S. Liu, J. Zhang, J. Zhang, R. Han and Q. Xu, *Chem. Eng. J.*, 259 (2015) 53.
29. Y. He, J. Sun, X. Wang and L. Wang, *Sensors and Actuators B: Chemical*, 221 (2015) 792.
30. W. Xiong, Q. Zhao, X. Li and L. Wang, *Particle & Particle Systems Characterization*, 33 (2016) 591.
31. W. Xiong, Q. Zhao, X. Li and L. Wang, *Particle & Particle Systems Characterization*, 33 (2016) 602.
32. Y. Wu, C. Chen and S. Liu, *Anal. Chem.*, 81 (2009) 1600.
33. G. Lai, F. Yan and H. Ju, *Anal. Chem.*, 81 (2009) 9730.
34. V. Salgueirino-Maceira, M.A. Correa-Duarte, M. Farle, A. López-Quintela, K. Sieradzki and R. Diaz, *Chemistry of Materials*, 18 (2006) 2701.
35. J. Gao, Z. Guo, F. Su, L. Gao, X. Pang, W. Cao, B. Du and Q. Wei, *Biosensors and Bioelectronics*, 63 (2015) 465.
36. C. Ruan, L. Yang and Y. Li, *Anal. Chem.*, 74 (2002) 4814.
37. G. Lai, H. Zhang, J. Yong and A. Yu, *Biosensors and Bioelectronics*, 47 (2013) 178.
38. S. Gomes-Filho, A. Dias, M. Silva, B. Silva and R. Dutra, *Microchemical Journal*, 109 (2013) 10.
39. X. Jia, X. Chen, J. Han, J. Ma and Z. Ma, *Biosensors and Bioelectronics*, 53 (2014) 65.
40. S. Palme, R.H. Christenson, S.A. Jortani, R.E. Ostlund, R. Kolm, G. Kopal and R.P. Laubender, *Clinical Biochemistry*, (2016) S0009.
41. S. Palme, R.H. Christenson, S.A. Jortani, R.E. Ostlund, R. Kolm, G. Kopal and R.P. Laubender, *European Respiratory Journal*, 48 (2016) PA3448.
42. N. Jeanblanc, S. Manetz, M. Liang, P. Choudhury, R. Varkey, E. Grant, M. Parker, K. Streicher, L. Greenlees and M. Datwyler, *European Respiratory Journal*, 46 (2015) PA3936.